

Article

Reaction Mechanism of Simultaneous Removal of H₂S and PH₃ Using Modified Manganese Slag Slurry

Jiacheng Bao ¹, Xialing Wang ¹, Kai Li ¹, Fei Wang ¹, Chi Wang ², Xin Song ¹, Xin Sun ^{1,*} and Ping Ning ^{1,*}

¹ Faculty of Environmental Science and Engineering, Kunming University of Science and Technology, Kunming 650500, China; jcBao@stu.kust.edu.cn (J.B.); wangxialing@stu.kust.edu.cn (X.W.); 20130203@kust.edu.cn (K.L.); 20192016@kust.edu.cn (F.W.); songxin@kust.edu.cn (X.S.)

² Faculty of Chemical Engineering, Kunming University of Science and Technology, Kunming 650500, China; 20150089@kust.edu.cn

* Correspondence: sunxin@kust.edu.cn (X.S.); ningping@kust.edu.cn (P.N.)

Received: 25 October 2020; Accepted: 26 November 2020; Published: 27 November 2020



Abstract: The presence of phosphine (PH₃) and hydrogen sulfide (H₂S) in industrial tail gas results in the difficulty of secondary utilization. Using waste solid as a wet absorbent to purify the H₂S and PH₃ is an attractive strategy with the achievement of “waste controlled by waste”. In this study, the reaction mechanism of simultaneously removing H₂S and PH₃ by modified manganese slag slurry was investigated. Through the acid leaching method for raw manganese slag and the solid–liquid separation subsequently, the liquid-phase part has a critical influence on removing H₂S and PH₃. Furthermore, simulation experiments using metal ions for modified manganese slag slurry were carried out to investigate the effect of varied metal ions on the removal of H₂S and PH₃. The results showed that Cu²⁺ and Al³⁺ have a promoting effect on H₂S and PH₃ conversion. In addition, the Cu²⁺ has liquid-phase catalytic oxidation for H₂S and PH₃ through the conversion of Cu(II) to Cu(I).

Keywords: phosphine; hydrogen sulfide; manganese slag; metal ions; reaction mechanism

1. Introduction

The presence of phosphine (PH₃) and hydrogen sulfide (H₂S) in industrial gases can result in reduced feed gas quality, excessive equipment corrosion, and catalyst deactivation and poisoning, limiting industrial gas recovery and utilization [1], especially yellow phosphorus off-gas. In addition, H₂S, as a highly toxic, corrosive gas, can not only cause air pollution but also eye irritation and breathing problems. Even exposure to small amounts of H₂S will pose a serious threat to humans [2]. Additionally, PH₃ may cause immediate death if one is exposed to a concentration level of 50 ppm, according to the National Institute for Occupational Safety and Health (NIOSH) [3]. Therefore, it is desirable to remove them from the point of view of the highly efficient use of industrial gases and human health.

Currently, the wet process has more advantages for simultaneously removing H₂S and PH₃ compared to the dry process, due to lower cost and easier preparation process [4,5]. However, the wet process for the removal of H₂S and PH₃ could rapidly consume oxidant, thus leading to a decrease in removal efficiency [4]. Hence, there is an urgent need to modify the traditional wet method to meet stricter environmental laws. In recent years, the use of metal ore, tailings, and metal smelting slag to remove industrial waste gas has attracted the attention of researchers [6–8]. Smelting slag contains a large number of transition metals such as Fe, Mn, and basic oxides, which could have been favorable for absorption of PH₃ and H₂S in the wet process due to the liquid phase catalytic oxidation ability of transition metals and higher alkalinity of basic oxides such as CaO, MgO, etc. The liquid catalytic

oxidation by transition metals can be favorable for the oxidation of gas pollutants, thus being conducive to absorbing H_2S or/and PH_3 [9–11]. At present, China has become the largest manganese producer, consumer, and exporter, and has emitted more than 2×10^6 tons of manganese slag (MS) every year, which mainly originate from the manganese metallurgy process. Piling manganese slag waste has caused color stain and pollution in the composition of soil and surface water and contaminated groundwater and rivers due to surface runoff [12]. Therefore, there is a pressing need to dispose of MS in a green and highly efficient manner. The chemical compositions of MS are rich in Mn-based oxides and contain a number of basic oxides, which make it possible to become a highly efficient absorbent for the removal of H_2S and PH_3 .

According to our previous studies [13], modified manganese slag (MS) slurry was used to remove H_2S and PH_3 and proved a great absorbent. However, a detailed investigation of the reaction mechanism was still lacking. Thus, our research extends the knowledge into the reaction mechanism of H_2S and PH_3 using modified MS slurry. In this paper, the emphasis was laid on the role of modified MS slurry in removing H_2S and PH_3 . In addition, to understand the liquid phase catalytic oxidation ability of modified MS slurry, we simulated the composition of MS slurry in the form of different metal salt solutions based on the actual composition of electrolytic MS. In addition, XPS (X-ray photoelectron spectrometer), IC (ion chromatography), and XRF (X-ray fluorescence) and XRD (X-ray diffraction) techniques were used to investigate the samples' surface information. Thus, a mechanism of simultaneous removal of PH_3 and H_2S using modified MS slurry was proposed.

2. Results and Discussion

2.1. Effect of Different Component Slurry after Acid Leaching on Simultaneous Removal of H_2S and PH_3

In order to investigate the mechanism of simultaneous removal of H_2S and PH_3 using modified MS slurry, the acid leaching method was used to treat the raw MS. Thus, the majority of soluble metal ions can be leached and transferred from the solid phase of raw MS to the aqueous solution. It can be seen from Figure 1 that XRD results show that the main mineral phases of raw MS were $3CaO \cdot SiO_2$ (C_3A), $2CaO \cdot SiO_2$ (C_2A), CaO , Al_2O_3 , and merwinite. These components were acid-soluble, which can be decomposed by the acid solution. Table 1 also shows that the main elements in raw MS were Si, Ca, and Mn. Thus, through acid leaching and then filtering, the active components mainly including metal ions could be removed from the raw MS.

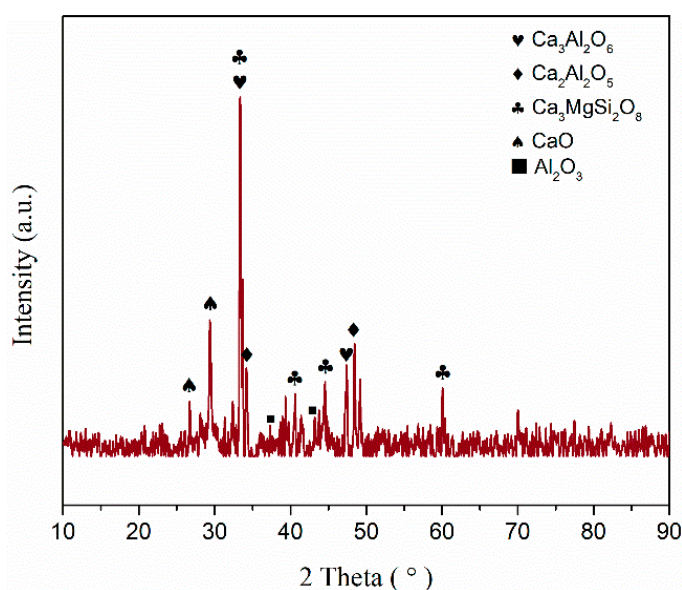


Figure 1. XRD pattern of raw manganese slag.

Table 1. XRF analysis of electrolytic manganese slag (wt.).

Element	Ca	Si	Mn	Al	Mg	S	O
Raw electrolytic manganese slag	25.54	13.09	11.33	4.80	3.54	1.87	37.48

As shown in Figure 2, the 100% H₂S removal efficiency of modified MS slurry (MS + CuSO₄ group) can maintain 7 h while the 65% PH₃ removal efficiency of modified MS slurry can maintain 5 h. In addition, the acid leaching residues and CuSO₄ slurry can only obtain around 7% H₂S removal efficiency and approximately 9% PH₃ removal efficiency. Compared with the simultaneous removal of H₂S and PH₃ by modified MS slurry, the acid leaching residue and CuSO₄ slurry obtained a poorer removal efficiency due to the consumption of active components after the acid leaching method. Additionally, the raw MS and Cu²⁺ have a synergistic effect on the removal of H₂S and PH₃. Thus, leached metal ions in slurry have a leading role in removing H₂S and PH₃. The mixture of MS and CuSO₄ slurry obtained the best PH₃ conversion efficiency while the effect of CuSO₄ solution was not obvious. According to our previous report [13], the increase in PH₃ conversion efficiency can be ascribed to the oxidation ability of Cu²⁺ and Mn²⁺ from MS, thus inhibiting the formation of CuS/Cu₂S.

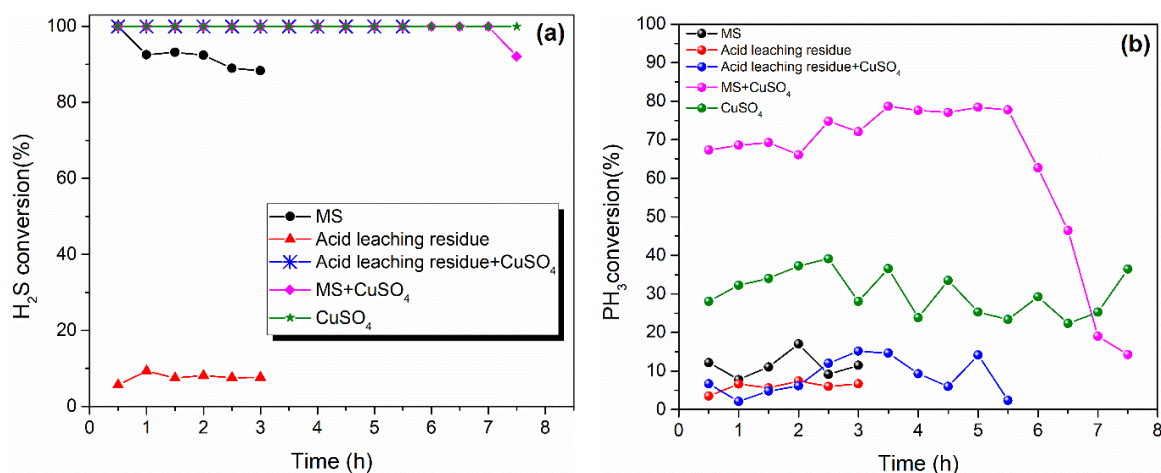


Figure 2. Effects of different component slurry after acid leaching on simultaneous removal of (a) H₂S and (b) PH₃ by manganese slag before and after acid leaching. Experimental conditions: H₂S concentration = 800 ppm; PH₃ concentration = 400 ppm; gas flow rate = 110 mL min⁻¹; reaction temperature = 35 °C; Oxygen content = 1 vol %; stirring rate = 800 r/min.

2.2. Effect of Simulated Modified MS Slurry on Simultaneous Removal of H₂S and PH₃

The metal ions leached from MS during the reaction period played a leading role in removing H₂S and PH₃. Thus, to gain more insight, the modified MS slurry was simulated in the form of metal salts based on the real component composition. The various simulated metal salts species (including metal nitrates, metal chlorides, and metal sulfates) were investigated and the simulated contents were listed in Table 2. The H₂S and PH₃ removal efficiency by simulated modified MS slurry is shown in Figure 3. The results showed that the three groups obtained a 100% H₂S conversion efficiency; whereas Group 3 (metal chlorides) obtained the higher PH₃ removal efficiency relative to those of the other groups, with the order being metal chlorides > metal nitrate > metal sulfates. In order to achieve a better understanding of the variation in PH₃ and H₂S conversion by different metal salts, the reaction products in aqueous solutions were detected by the IC method. The IC results, as shown in Figure 4, showed that the generated PO₃⁻ and SO₄²⁻ concentrations in Group 3 increased with the reaction proceeding, which indicated that the H₂S and PH₃ could be converted to PO₃⁻ and SO₄²⁻, respectively. Thus, the addition of metal sulfates inhibited higher H₂S and PH₃ conversion efficiency because the generation of SO₄²⁻ was accelerated and inhibited the oxidation of PH₃ when the copper concentration

was at relatively high concentration, according to our previous study [13]. In other words, more sulfates existing in the solution led to lower PH_3 conversion efficiency. Hence, the metal chloride was chosen for the following experiments.

Table 2. Composition of simulated modified manganese slag slurry.

Samples	Composition (wt.%), Total Mass = 3 g, Balanced in SiO_2				
	Ca^{2+}	Mg^{2+}	Mn^{2+}	Al^{3+}	Extra Added Cu^{2+}
Group 1 (metal nitrates)	25.54	3.54	11.33	4.80	0.01 mol
Group 2 (metal chlorides)	25.54	3.54	11.33	4.80	0.01 mol
Group 3 (metal sulfates)	25.54	3.54	11.33	4.80	0.01 mol

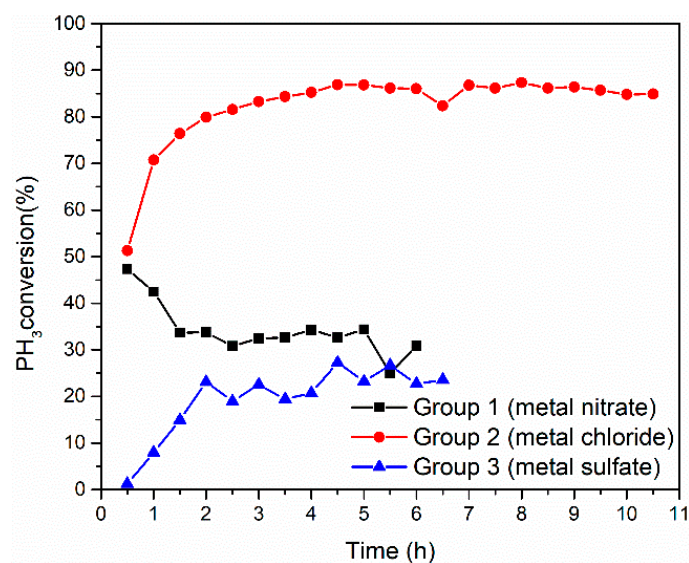


Figure 3. Effect of different simulated modified manganese slag (MS) slurry on simultaneous removal of H_2S and PH_3 by manganese slag before and after acid leaching. Experimental conditions: H_2S concentration = 800 ppm; PH_3 concentration = 400 ppm; gas flow rate = 110 mL min^{-1} ; reaction temperature = $35 \text{ }^\circ\text{C}$; Oxygen content = 1 vol %; stirring rate = 800 r/min.

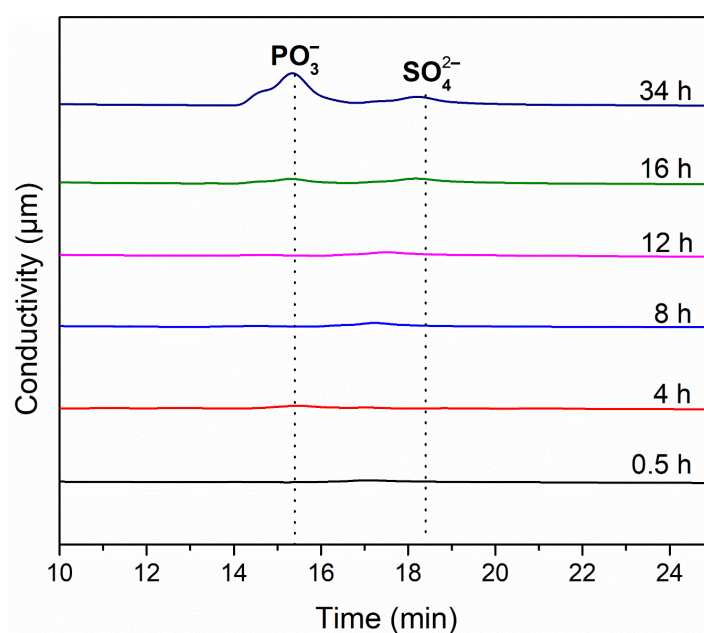


Figure 4. Ion concentration in Group 3 (metal chloride) as a function of time (50× dilution).

2.3. Effect of Single and Multi-Metal Ions on Simultaneous Removal of H₂S and PH₃

To further explore the role of metal ions in removing H₂S and PH₃, we provide a series of experiments to examine the effect of metal ions on H₂S and PH₃ removal. It can be seen from Figure 5 that all groups can achieve 100% H₂S removal efficiency. The highest PH₃ conversion efficiency of Cu²⁺ + Al³⁺, Cu²⁺ + Ca²⁺, Cu²⁺ + Mg²⁺, and Cu²⁺ + Mn²⁺ were 95.52%, 89.45%, 87.43%, and 81.63%, respectively. The Al³⁺ + Cu²⁺ group obtained higher PH₃ conversion efficiency relative to that of Cu²⁺ alone, which indicated that the Al³⁺ and Cu²⁺ have a synergistic effect on PH₃ removal. The addition of Mg²⁺, Ca²⁺, and Mn²⁺ slightly reduced the PH₃ conversion efficiency compared to those of the Cu²⁺ group and Al³⁺ + Cu²⁺ group. Thus, the analysis emphasis was laid on the Al³⁺ + Cu²⁺ group, and the reaction products in long-term experiments are analyzed in the next section (Section 2.4).

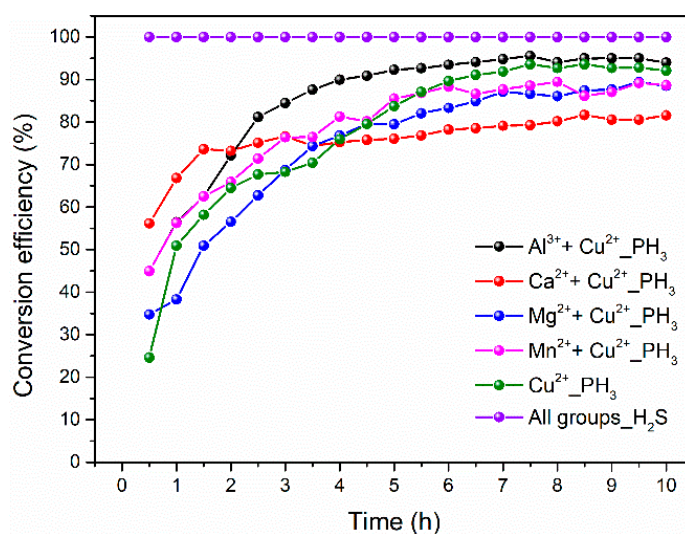


Figure 5. Effect of different single and multi-metal ions (metal chlorides) on simultaneous removal of H₂S and PH₃. Experimental conditions: H₂S concentration = 800 ppm; PH₃ concentration = 400 ppm; gas flow rate = 110 mL min⁻¹; reaction temperature = 35 °C; Oxygen content = 1 vol %; stirring rate = 800 r/min.

2.4. Reaction Mechanism of Metal Ions to Simultaneous Removal of H₂S and PH₃

To understand the effect of Al³⁺ combined with Cu²⁺ on simultaneous removal of H₂S and PH₃, the long-term experiments were carried out and the variation in the pH value of solution, solid or aqueous products is analyzed in this section. For the Cu²⁺ group, Figure 6a shows that the PH₃ conversion efficiency increased initially and then decreased with the reaction proceeding, accompanied by a gradual decrease in the pH value. The XRD results in Figure 6b indicate that the main reaction product was CuS, Cu₈S₅, and CuCl, which resulted from the reaction between H₂S and Cu²⁺ (Equation (1)). Meanwhile, the H⁺ ion was increased, thereby leading to a decrease in pH value. The Al³⁺ + Cu²⁺ group showed a similar conversion trend for H₂S and PH₃. However, the reaction products of the Al³⁺ + Cu²⁺ group became different. It can be seen from Figure 6d that the Al₂(SO₄)₃, CuSO₄, Cu₄(SO₄)(OH)₆·2H₂O, and CuS were the main reaction products for removing H₂S while AlPO₃, AlP, and Cu₅O₂(PO₄)₂ were the main reaction products for removing PH₃. When Al³⁺ was added into the solution, the pH value slowly decreased during 5 h of initial reaction time, which indicated that Al³⁺ could inhibit the rapid decline of pH value, although the pH value subsequently decreased dramatically.



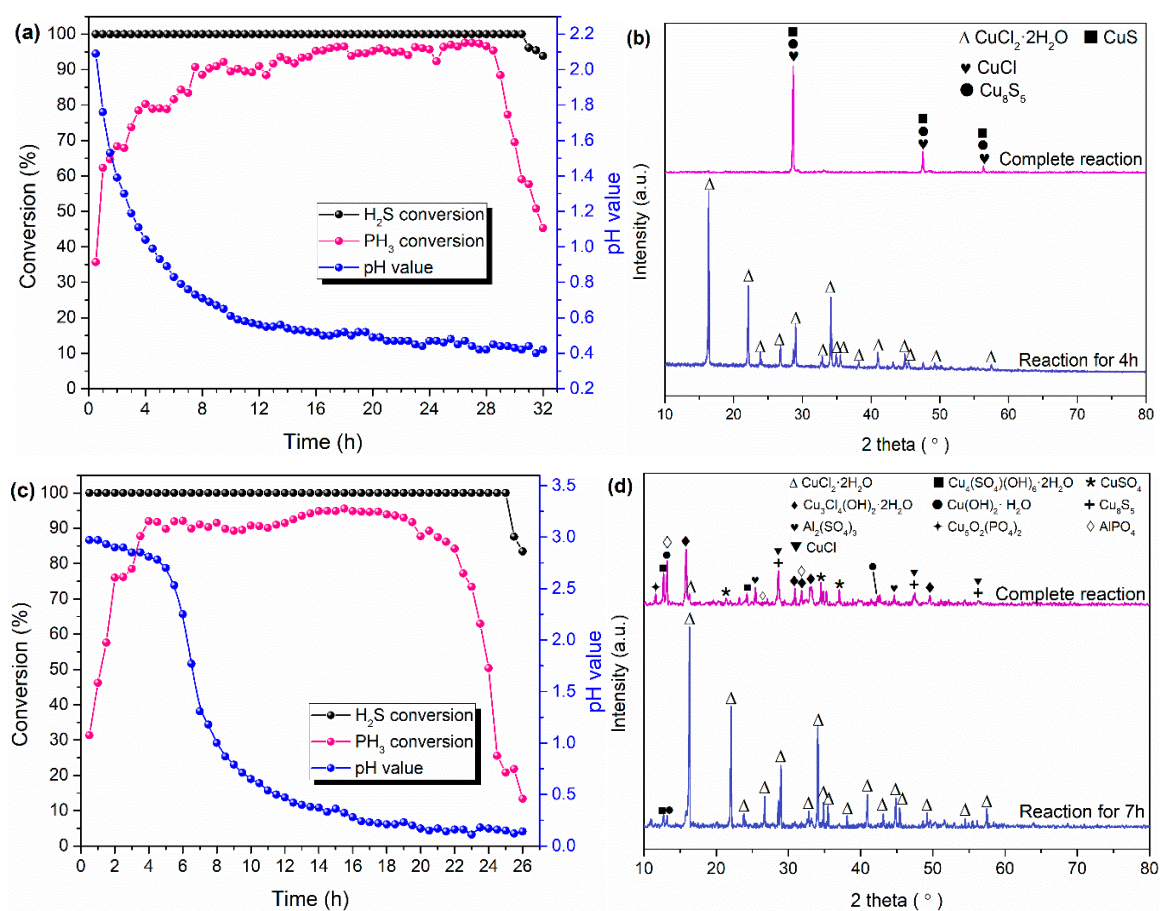


Figure 6. Variation in pH value of (a) Cu²⁺ group and (c) Al³⁺ + Cu²⁺ group as a function of time. XRD patterns of reaction process of (b) Cu²⁺ group and (d) Al³⁺ + Cu²⁺ group. Experimental conditions: H₂S concentration = 800 ppm; PH₃ concentration = 400 ppm; gas flow rate = 110 mL min⁻¹; reaction temperature = 35 °C; Oxygen content = 1 vol %; stirring rate = 800 r/min.

To gain more insight, we conducted several XPS studies for the reaction products of the Cu²⁺ group and Al³⁺ + Cu²⁺ groups with the reaction proceeding. For the Al³⁺ + Cu²⁺ group, as shown in Figure 7a, the binding energy (B. E.) centered at about 159.4 eV for S 2p_{3/2} could be attributed to S²⁻ [14], which indicated that CuS was generated in the Al³⁺ + Cu²⁺ group. In addition, the B. E. located at 164.2 eV may be ascribed to polysulfide species [15], which indicated that CuS/Cu₈S₅ was oxidized in the existence of oxygen. With the reaction further proceeding, the sulfate was formed as evidence that the B. E. of 169.8 eV appeared [16] and the sulfate content further increased from 7 h to complete reaction, which indicated that CuS was further oxidized to CuSO₄ by oxygen in the presence of the water environment [17]. This was consistent with the XRD results as shown in Figure 6d. For the Cu²⁺ group, the variation in S valence state in the initial reaction period was similar to the Al³⁺ + Cu²⁺ group. However, with further increase of the reaction time, the content of the polysulfide species (53.2%, calculated by XPS data as shown in Table 3) was the same as the sulfate content (46.8%); whereas the sulfate content (91.4%) was dominant in the Al³⁺ + Cu²⁺ group. This can be explained by noting that the addition of Al³⁺ could effectively accelerate the CuS oxidation, thus generating more sulfate species.

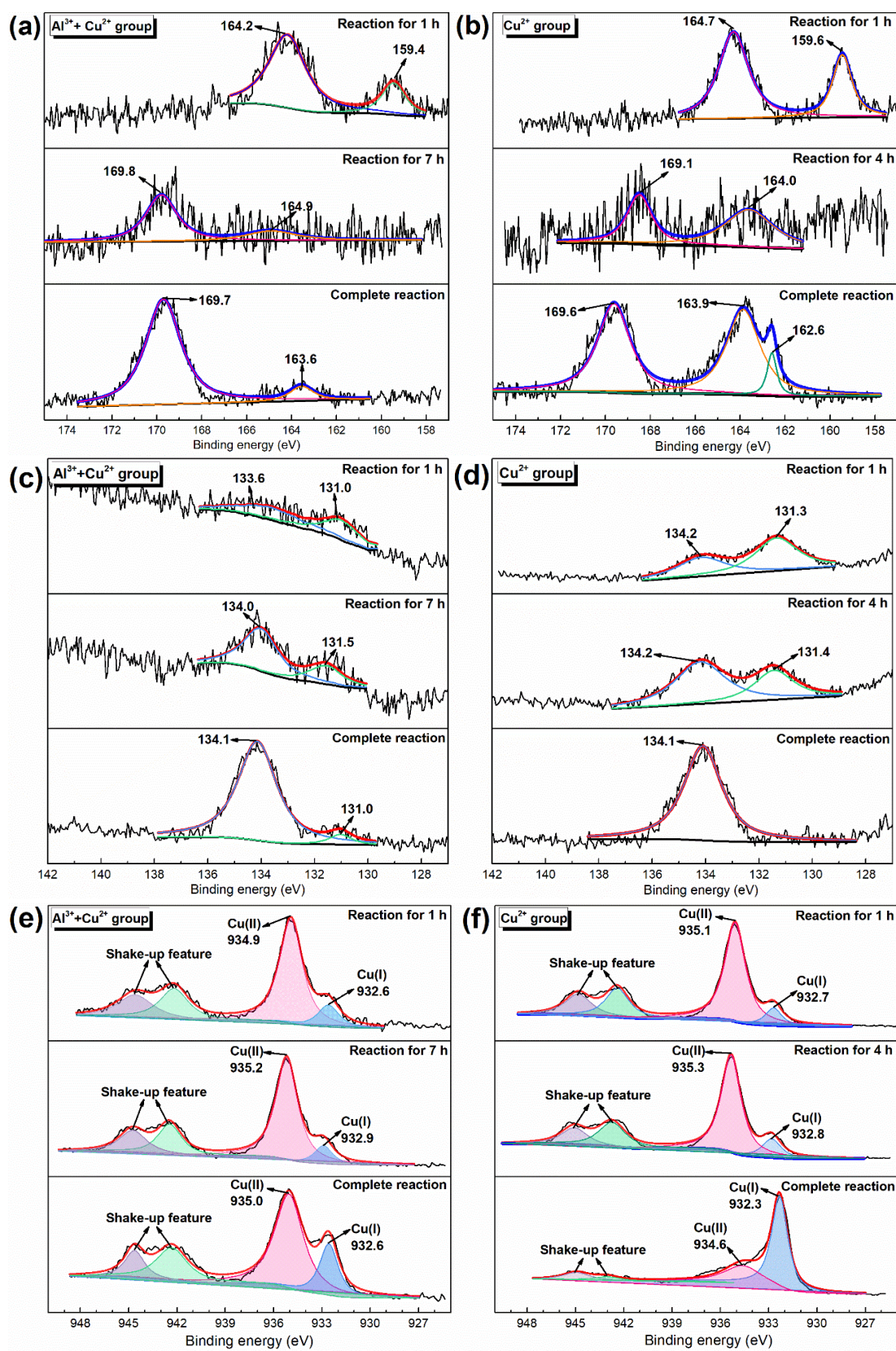


Figure 7. XPS spectra of $\text{Al}^{3+} + \text{Cu}^{2+}$ group and Cu^{2+} group with different reaction time for surveys of (a,b) S 2p, (c,d) P 2p, and (e,f) Cu 2p.

Table 3. XPS data of Al³⁺ + Cu²⁺ group and Cu²⁺ group with different reaction time for surveys of S 2p; P 2p, and Cu 2p.

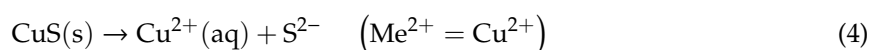
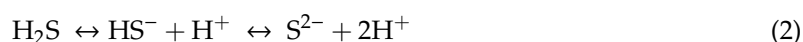
Sample	Element	Parameter	Reaction Time						
			1 h	4 h	Complete Reaction				
Cu ²⁺ Group	S	Position (eV)	164.7	159.6	169.1	164.0	169.6	163.9	162.6
		Atomic ratio (%)	68.2	31.9	40.4	59.6	46.8	46.5	6.7
		Substance	S _n ¹	S ²⁻	SO ₄ ²⁻	S	SO ₄ ²⁻	S _n	S _n
	P	Position (eV)	134.2	131.3	134.2	131.4	134.1		
		Atomic ratio (%)	39.9	60.1	64.7	35.3	100.0		
		Substance	PO ₄ ³⁻	P ³⁻	PO ₄ ³⁻	P ³⁻	PO ₄ ³⁻		
	Cu	Position (eV)	935.1	932.7	932.8	935.3	932.3	934.6	
		Atomic ratio (%)	87.9	12.1	15.2	84.8	70.2	29.8	
		Substance	CuSO ₄	CuS	CuS	CuSO ₄	CuS	CuSO ₄	
Al ³⁺ + Cu ²⁺ Group	S	Position (eV)	164.2	159.4	169.8	164.9	169.7	163.6	
		Atomic ratio (%)	78.4	21.6	74.2	25.8	91.4	8.6	
		Substance	S _n	S ²⁻	SO ₄ ²⁻	S	S _n	S _n	
	P	Position (eV)	133.6	131.0	134.0	131.5	134.1	131.0	
		Atomic ratio (%)	51.7	48.3	69.8	30.2	94.4	5.6	
		Substance	PO ₄ ³⁻	P ³⁻	PO ₄ ³⁻	P ³⁻	PO ₄ ³⁻	P ³⁻	
	Cu	Position (eV)	934.9	932.6	935.2	932.9	935.0	932.6	
		Atomic ratio (%)	83.5	16.5	86.5	13.5	73.6	26.4	
		Substance	Cu(II)	Cu(I)	Cu(II)	Cu(I)	Cu(II)	Cu(I)	

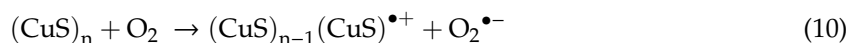
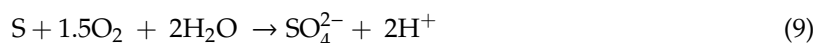
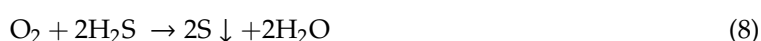
¹ S_n refers to the polysulfide species.

As shown in Figure 7c, when the Al³⁺ + Cu²⁺ group reacted for 1 h, phosphate was formed, since the peak at 134.6 eV could be attributed to PO₄³⁻ while the B. E. of 131.0 eV may be ascribed to P³⁻. With an increase in reaction time, the PO₄³⁻ content increased from 51.7% to 69.8%, up to 94.4% in the final. The variation of the P valence state in the Cu²⁺ group as shown in Figure 7d was the same as for the Al³⁺ + Cu²⁺ group; but the generation rate of phosphate in the Cu²⁺ group was slower than that of the Al³⁺ + Cu²⁺ group. When the reaction time was for 1 h, the relative phosphate content in the Cu²⁺ group was 39.9%, thus leading to a slower increased PH₃ conversion efficiency than the Cu²⁺ group. The faster conversion of PH₃ to phosphate resulted in accelerated PH₃ absorption in the initial period of reaction.

It can be seen from Figure 7e that the B. E. located at around 934.9 and 932.6 eV in the Al³⁺ + Cu²⁺ group could be attributed to Cu(II) and Cu(I), respectively [18]. The relative Cu²⁺ content in the Al³⁺ + Cu²⁺ group was 83.5% for 1 h of reaction time and then decreased to 73.6% until the complete reaction, which indicated that part of Cu²⁺ was converted to Cu⁺ as evidenced by the formation of CuCl and Cu₈S₅ by the XRD technique. From Figure 7f, it can be seen that the ratio of Cu(II)/Cu(I) in the Cu²⁺ group decreased dramatically relative to the Al³⁺ + Cu²⁺ group, which indicated that Cu²⁺ ion had a liquid-phase catalytic oxidation effect on removing H₂S and PH₃ through variation in the valence state of Cu²⁺ to Cu⁺.

Based on the above analysis, the metal ions played a leading role in removing H₂S and PH₃. The reaction process can be summarized as follows (Equations (2)–(13)):





3. Materials and Methods

3.1. Materials

The manganese slag samples were collected from Wenshan, China. The electrolytic manganese slag is firstly dried at 105 °C in the oven for 12 h, then mechanically ground by ball mill and sieved to 200 mesh (74 μm) for use. The standard gases include N₂ (≥99.99%), H₂S/N₂ (1.00% H₂S, v/v), PH₃/N₂ (1.00% PH₃, v/v), and O₂ (≥99.99%), all of which were purchased from Dalian Special Gases Co., Ltd., Dalian, China.

3.2. Acid Leaching Procedure and Preparation of Modified MS Slurry

First, the electrolytic manganese slag was weighed and transferred into a three-necked flask. Then, 2 mol L⁻¹ hydrochloric acid solution was taken into the three-necked flask with the connecting condensing device. The solid-to-liquid ratio of the slag to the acid solution was 1:6. The acid leaching temperature was set at 100 °C for 60 min. After acid leaching, the acid-leached solution was filtered. Then, filter residue and filtrate were obtained. The obtained filter residue was named as acid leaching residue. The acid leaching residue was then mixed with deionized water to obtain a 40 mL acid leaching residue slurry. Furthermore, the acid leaching residue was mixed with 0.01 mol CuSO₄, named as acid leaching residue + CuSO₄. The mixture of acid leaching residue and CuSO₄ was added into 40 mL deionized water to prepare the acid leaching residue + CuSO₄ slurry. The modified MS slurry was obtained by a mixture of 3 g MS, 40 mL deionized water, and 0.01 mol CuSO₄, named MS + CuSO₄. In addition, the 3 g of raw MS was added to 40 mL deionized water to prepare the raw MS slurry, named MS. The CuSO₄ solution also was prepared by adding a mixture of 40 mL deionized water and 0.01 mol CuSO₄, named CuSO₄.

3.3. Analytical Method

The solid samples were characterized by XPS technology to obtain the information of S 2p, P 2p, and Cu 2p that were measured by the ESCALAB 250 X-ray photoelectron spectrometer (Thermo Fisher Scientific, Waltham, MA, USA) with a resolution of 0.45 eV (Ag) and 0.82 eV (PET). The sensitivity of the instrument is 180 kbps (200 μm, 0.5 eV). The anions in the solutions were detected by ICS-600 (Thermo Fisher Scientific, Waltham, MA, USA). The ion chromatography is equipped with an AS12A anion separation column consisting of sodium carbonate and sodium bicarbonate. The instrument is turned on for 1–2 h, and the background conductance is less than 30 μs to start measurement. XRD method was used to determine the phase structure of the solid samples prior and after H₂S and PH₃ absorption experiments by a D/MAX-2200 X-ray diffractometer (Rigaku, Tokyo, Japan) with Cu Kα ray, at a voltage of 36 kV, at a current of 30 mA, with scanning range between 10 and 90°, and at a scanning speed of 5°/min.

3.4. Catalytic Activity Test

The experiment device for evaluating the activity of the remover is shown in Figure 8. The simulated flue gas consists of O₂, H₂S, PH₃, and N₂, all of which were supplied by gas cylinders (1a–1d), and their concentration were 1 vol %, 800 ppm (parts per million by volume), 400 ppm, respectively, with a total gas flow rate of 110 mL/min. The gas flow in each gas path is controlled by mass flow controllers (2) (Beijing Seven-Star Electronics Co., Ltd., Beijing, China) with a digital display (4) (Beijing Seven-star Electronics Co., Ltd., Beijing, China), then all of the gases were mixed in the mixing tank (5) (J.K Fluid Technology, Jiaxing, China). The mixed gas will reach the desired concentration by adjusting the mass flow controllers, and be analyzed by gas chromatography (6) (FULI-9790II gas chromatography, FULI Instrument Co., Ltd., Taizhou, China). Then, the mixed gas passes through three-necked flask (10) combined with the constant temperature magnetic stirrer (DF-101S, INESA Scientific Instrument Co., Ltd., Shanghai, China), contacting the prepared modified manganese slag slurry in which mixed gas will react with the slurry. During the reaction process, the pH value of slurry was measured by pH meter (PHS-3C, INESA Scientific Instrument Co., Ltd., Shanghai, China). Moreover, the tail gas will first be analyzed by a gas chromatography and then be removed in the tail gas treatment system (9) (scrubbed by the 5 wt.% KMnO₄ solution with 5 wt.% H₂SO₄).

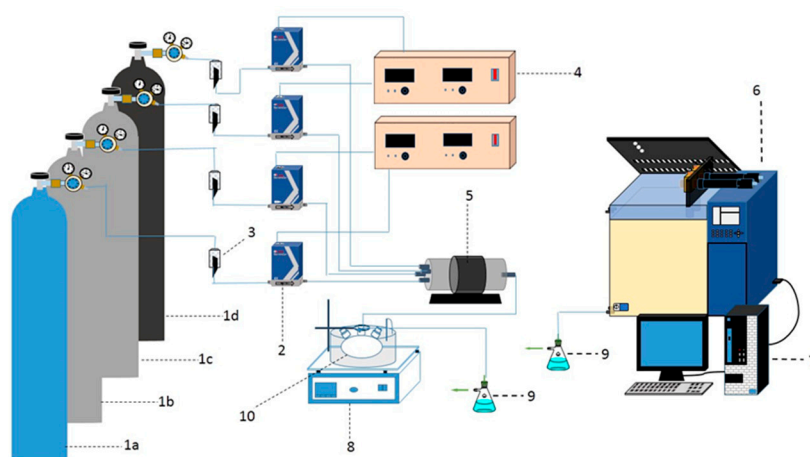


Figure 8. Experimental device diagram of extractant activity evaluation. 1a, 99.99% O₂ cylinder gas; 1b, 1 vol % H₂S cylinder gas; 1c, 1 vol % PH₃ cylinder gas; 1d, 99.99 vol % N₂ cylinder gas; 2, mass flow meter; 3, on-off valve; 4, digital display; 5, gas mixing tank; 6, FULI-9790II gas chromatography; 7, data analysis; 8, constant temperature magnetic stirrer; 9, exhaust gas absorption bottle; 10, three-necked flask.

The calculation method for the conversion efficiency of PH₃ and H₂S is shown in Equation (14).

$$\text{PH}_3(\text{H}_2\text{S}) \text{ conversion efficiency } \% = \frac{\text{PH}_3(\text{H}_2\text{S})_{\text{inlet}} - \text{PH}_3(\text{H}_2\text{S})_{\text{outlet}}}{\text{PH}_3(\text{H}_2\text{S})_{\text{inlet}}} \times 100 \quad (14)$$

where PH₃ inlet and H₂S inlet refer to the inlet concentrations of PH₃ and H₂S at the initial of the reactor, respectively, in mg/m³; and PH₃ outlet and H₂S outlet refer to the outlet concentrations of PH₃ and H₂S at the end of the reactor, respectively, in mg/m³.

4. Conclusions

In this study, modified MS slurry was systematically carried out toward simultaneously removing H₂S and PH₃. On the basis of different characterization techniques, we investigated the reaction mechanism of removing H₂S and PH₃ by modified MS slurry. The main findings of this study are as follows:

- (1) Through acid leaching experiments, the liquid-phase part after filtration has a leading role in removing H₂S and PH₃. The highest PH₃ conversion efficiency of leaching residue slurry + CuSO₄ group can only obtain 15.14%, which indicated that the main active components were consumed by the acid leaching method.
- (2) By simulation of the modified MS slurry with metal ions based on real chemical composition, the catalytic activity for H₂S and PH₃ is relative to the types of metal salts, with the order being metal chlorides > metal nitrates > metal sulfates. All of the metal salts can obtain 100% H₂S removal efficiency. In addition, the metal chlorides can maintain above 70% PH₃ conversion efficiency for 10.5 h and the highest PH₃ conversion efficiency was 86.85%; whereas the highest PH₃ removal efficiency of the metal nitrates and metal sulfates can only obtain 47.36% and 27.24%, respectively. Furthermore, Al³⁺ and Cu²⁺ has a synergistic effect on removing H₂S and PH₃ compared to Ca²⁺, Mg²⁺, and Mn²⁺ combined with Cu²⁺ groups.
- (3) H₂S was oxidized to element S and sulfate due to the reaction between Cu²⁺ and H₂S and part of the H₂S oxidation by O₂, while the PH₃ was oxidized to PO₄³⁻ by liquid-phase catalytic oxidation of metal ions with the conversion of Cu²⁺ to Cu⁺.
- (4) The best PH₃ and H₂S conversion efficiency was obtained by the modified MS slurry (MS + CuSO₄), and the maximum removal efficiency of H₂S and PH₃ were 100% and ~78%, respectively. The simple modification process for raw MS through adding Cu²⁺ can effectively improve the H₂S and PH₃ conversion relative to fresh MS, which can be attributed to the synergistic effect of different metal ions. However, the added Cu²⁺ in the modified MS slurry would be consumed by conversion of Cu²⁺ to CuS/Cu₂S, thereby leading to the deactivation of modified MS slurry.

Author Contributions: J.B. and X.W. contributed equally. Conceptualization, X.S. (Xin Sun) and P.N.; methodology, X.S. (Xin Sun); software, C.W. and X.S. (Xin Song); validation, X.W.; formal analysis, J.B.; investigation, X.W.; resources, X.S. (Xin Sun), K.L., and P.N.; data curation, J.B.; writing—original draft preparation, J.B.; writing—review and editing, J.B.; visualization, J.B.; supervision, X.S. (Xin Sun); funding acquisition, X.S. (Xin Sun), K.L., F.W., and P.N. All authors have read and agreed to the published version of the manuscript.

Funding: This research was funded by the National Natural Science Foundation of China (grant 51708266, 51968034, 21667015, and 41807373) and the National Key R&D Program of China (grant 2018YFC0213400, 2018YFC1900305).

Conflicts of Interest: The authors declare no conflict of interest.

References

1. Ma, Y.; Wang, X.; Ning, P.; Cheng, C.; Wang, F.; Wang, L.; Lin, Y.; Yu, Y. Simultaneous Removal of PH₃, H₂S, and Dust by Corona Discharge. *Energ. Fuel* **2016**, *30*, 9580–9588. [[CrossRef](#)]
2. Zhang, C.; Cheng, R.H.; Li, S.G.; Liu, C.; Chang, J.; Liu, H. Controls on Hydrogen Sulfide Formation and Techniques for Its Treatment in the Binchang Xiaozhuang Coal Mine, China. *Energy Fuels* **2019**, *33*, 266–275. [[CrossRef](#)]
3. Chang, S.-M.; Hsu, Y.-Y.; Chan, T.-S. Chemical Capture of Phosphine by a Sol-Gel-Derived Cu/TiO₂ Adsorbent—Interaction Mechanisms. *J. Phys. Chem. C* **2011**, *115*, 2005–2013. [[CrossRef](#)]
4. Qu, G.F.; Zhao, Q.; Jian, R.L.; Wang, J.Y.; Liu, D.X.; Ning, P. Mechanism of PH₃ absorption by CuTILs/H₂O two-liquid phase system. *Sep. Purif. Technol.* **2017**, *187*, 255–263. [[CrossRef](#)]
5. Govindan, M.; Chung, S.J.; Jang, J.W.; Moon, I.S. Removal of hydrogen sulfide through an electrochemically assisted scrubbing process using an active Co (III) catalyst at low temperatures. *Chem. Eng. J.* **2012**, *209*, 601–606. [[CrossRef](#)]
6. Fois, E.; Lallai, A.; Mura, G. Sulfur dioxide absorption in a bubbling reactor with suspensions of Bayer red mud. *Ind. Eng. Chem. Res.* **2007**, *46*, 6770–6776. [[CrossRef](#)]
7. Montes-Moran, M.A.; Concheso, A.; Canals-Battle, C.; Aguirre, N.V.; Ania, C.O.; Martin, M.J.; Masaguer, V. Linz-Donawitz Steel Slag for the Removal of Hydrogen Sulfide at Room Temperature. *Environ. Sci. Technol.* **2012**, *46*, 8992–8997. [[CrossRef](#)] [[PubMed](#)]

8. Kim, K.; Asaoka, S.; Yamamoto, T.; Hayakawa, S.; Takeda, K.; Katayama, M.; Onoue, T. Mechanisms of Hydrogen Sulfide Removal with Steel Making Slag. *Environ. Sci. Technol.* **2012**, *46*, 10169–10174. [[CrossRef](#)] [[PubMed](#)]
9. Lee, E.K.; Jung, K.D.; Joo, O.S.; Shul, Y.G. Liquid-phase oxidation of hydrogen sulfide to sulfur over CuO/MgO catalyst. *React. Kinet. Catal. Lett.* **2005**, *87*, 115–120. [[CrossRef](#)]
10. Monakhov, K.Y.; Gourlaouen, C. On the Insertion of ML_2 ($M = Ni, Pd, Pt$; $L = PH_3$) into the E-Bi Bond ($E = C, Si, Ge, Sn, Pb$) of a Bicyclo [1.1.1] Pentane Motif: A Case for a Carbenoid-Stabilized Bi(0) Species? *Organometallics* **2012**, *31*, 4415–4428. [[CrossRef](#)]
11. Goncharova, L.V.; Clowes, S.K.; Fogg, R.R.; Ermakov, A.V.; Hinch, B.J. Phosphine adsorption and the production of phosphide phases on Cu(001). *Surf. Sci.* **2002**, *515*, 553–566. [[CrossRef](#)]
12. Chen, H.; Feng, Y.; Suo, N.; Long, Y.; Li, X.; Shi, Y.; Yu, Y. Preparation of particle electrodes from manganese slag and its degradation performance for salicylic acid in the three-dimensional electrode reactor (TDE). *Chemosphere* **2019**, *216*, 281–288. [[CrossRef](#)] [[PubMed](#)]
13. Sun, L.N.; Song, X.; Li, K.; Wang, C.; Sun, X.; Ning, P.; Huang, H.B. Preparation of modified manganese slag slurry for removal of hydrogen sulphide and phosphine. *Can. J. Chem. Eng.* **2020**, *98*, 1534–1542. [[CrossRef](#)]
14. Fleet, M.E.; Harmer, S.L.; Liu, X.; Nesbitt, H.W. Polarized X-ray absorption spectroscopy and XPS of TiS_3 : S K- and Ti L-edge XANES and S and Ti 2p XPS. *Surf. Sci.* **2005**, *584*, 133–145. [[CrossRef](#)]
15. Mikhlin, Y.; Likhatski, M.; Tomashevich, Y.; Romanchenko, A.; Erenburg, S.; Trubina, S. XAS and XPS examination of the Au-S nanostructures produced via the reduction of aqueous gold(III) by sulfide ions. *J. Electron Spectrosc. Relat. Phenom.* **2010**, *177*, 24–29. [[CrossRef](#)]
16. Beattie, D.A.; Arcifa, A.; Delcheva, I.; Le Cerf, B.A.; MacWilliams, S.V.; Rossi, A.; Krasowska, M. Adsorption of ionic liquids onto silver studied by XPS. *Colloid. Surface A* **2018**, *544*, 78–85. [[CrossRef](#)]
17. Wu, H.B.; Or, V.W.; Gonzalez-Calzada, S.; Grassian, V.H. CuS nanoparticles in humid environments: adsorbed water enhances the transformation of CuS to $CuSO_4$. *Nanoscale* **2020**, *12*, 19350–19358. [[CrossRef](#)] [[PubMed](#)]
18. Liu, H.Y.; Xie, J.W.; Liu, P.; Dai, B. Effect of Cu^+/Cu^{2+} Ratio on the Catalytic Behavior of Anhydrous Nieuwland Catalyst during Dimerization of Acetylene. *Catalysts* **2016**, *6*, 120. [[CrossRef](#)]

Publisher's Note: MDPI stays neutral with regard to jurisdictional claims in published maps and institutional affiliations.



© 2020 by the authors. Licensee MDPI, Basel, Switzerland. This article is an open access article distributed under the terms and conditions of the Creative Commons Attribution (CC BY) license (<http://creativecommons.org/licenses/by/4.0/>).